Rotationally Adaptive Flight Test Surface

Final Report

by

Ron Barrett
Assistant Professor of Aerospace Engineering
Auburn University, AL 36849
(334) 844-6825 (office) -6832 (lab) -6803 (FAX) rbarrett@eng.auburn.edu

for

Mr. David Voracek
National Aeronautics and Space Administration
Dryden Flight Research Center
Warehouse #6, Bldg. 4876
Edwards, California 93524
(805) 258-2463

under contract number: NCC4-103

15 April 1999

Abstract

Research on a new design of flutter exciter vane using adaptive materials was conducted. This novel design is based on all-moving aerodynamic surface technology and consists of a structurally stiff main spar, a series of piezoelectric actuator elements and an aerodynamic shell which is pivoted around the main spar. The work was built upon the current missile-type all-moving surface designs and change them so they are better suited for flutter excitation through the transonic flight regime. The first portion of research will be centered on aerodynamic and structural modeling of the system. USAF DatCom and vortex lattice codes was used to capture the fundamental aerodynamics of the vane. Finite element codes and laminated plate theory and virtual work analyses will be used to structurally model the aerodynamic vane and wing tip. Following the basic modeling, a flutter test vane was designed. Each component within the structure was designed to meet the design loads. After the design loads are met, then the deflections will be maximized and the internal structure will be laid out. In addition to the structure, a basic electrical control network will be designed which will be capable of driving a scaled exciter vane. The third and final stage of main investigation involved the fabrication of a 1/4 scale vane. This scaled vane was used to verify kinematics and structural mechanics theories on all-moving actuation. Following assembly, a series of bench tests was conducted to determine frequency response, electrical characteristics, mechanical and kinematic properties. Test results indicate peak-to-peak deflections of 1.1 deg with a corner frequency of just over 130 Hz.

1. Background of the Problem or Opportunity

During the past decade, great strides have been made in the area of flight control through adaptive materials. Many of these systems have been centered on shape-memory alloy, piezoceramic and magnetostrictive actuation of flight control surfaces. Some of the earliest groundbreaking work was performed on active vibration control.[1] These early studies were rapidly followed by innovations in modeling which demonstrated that relatively simple laminated plate theories could be used to accurately model the performance of many types of adaptive structures.[2,3] These studies paved the way for attempts at flight control. Through aeroelastic effects, it was thought that small active deflections could be magnified to produce usable deflections.[4-6] At about the same time as the early active aeroelastic estimations, it was discovered that twist could be directly imparted to uncoupled structures by piezoceramic elements. This discovery of directionally attached piezoelectric (DAP) elements opened the door to a host of aerodynamic control devices.[7-13]

Modifications to the conventional DAP structures were made to include aeroservoelastic deformations. Several studies showed that small deflections could be effectively magnified just like earlier conventional adaptive structures approaches.[14] One of the first application-oriented studies used a new concept dubbed active free-spar torque-plate missile fins. These novel fins employed the torque plates and DAP elements of earlier studies, but, for the first time, they were applied to practical flight vehicles.[15-17] These torque-plate fins provided moderate deflections with moderate forces, but for some flight regimes, smaller pitching moments are common. In particular, the low subsonic flight regime yields nearly negligible pitching moments about the aerodynamic center. Accordingly, another family of adaptive aerostructure actuators was developed. These Flexspar actuators provided the highest recorded active pitch deflections for flight control purposes.[18-21]

Although fine for the low subsonic flight regime, these actuators very quickly become saturated by pitching moments at transonic Mach numbers. The center of pressure shift simply overpowers the relatively weak adaptive structures within the shell. To counter this adverse property, yet another class of (unpublished) actuators were developed specifically for the transonic flight regime. These rotationally active linear actuators (RALA) are capable of utilizing up to 95% of the active strain energy of the piezoceramics (rather than the 10 to 40% which is captured by other methods). Because the strain energy capture rate is so much higher, the moment-deflection work

zones are nearly an order of magnitude greater than preceding actuators. As with all new approaches, however, a penalty is paid in total deflection angle. Accordingly, these new actuators are high moment, low displacement devices.[22]

As the development of active aerostructures has progressed, new innovations in the flutter flight test devices have also made great strides. Numerous flutter exciters which are based on inertial, aerodynamic and pyrotechnic forces have been fabricated and used.[23-27] One of the most modern devices circumvents many of the difficulties which is found with each of the earlier systems. This rotating cylinder-based structural excitation system has been shown to provide adequate levels of excitation at the desired frequency ranges and moderate power consumption levels.[28] However, there exists an opportunity to use the adaptive aerodynamic flight control device technology to improve upon the performance levels which were obtained by the rotating cylinder-based structural excitation system.

Because adaptive elements are much more efficient than conventional electromechanical actuators, the power consumption of the system will be significantly reduced. Also, the solid state nature of such actuators generally widens the frequency response of the system. An added benefit which is important to specific structural excitation schemes is the ability to use non-sinusoidal and superimposed waveforms. The non-sinusoidal waveform input will place pseudo-step force inputs into the aircraft. Such a square-wave excitation scheme will tend to induce higher structural modes. The superimposed waveform capability will allow for testing structural interactions and cross-couplings. Such tests may be conducted with a steady excitation of one structural mode (second bending for example) while simultaneously performing a frequency sweep in the vicinity of another mode (first torsion for example). Because the system is capable of step and superimposed responses, a white noise test signal may be fed to the fin. Such a white noise signal may be used in conjunction with atmospheric turbulence to drive high structural modes. Another benefit of such a system is that it will occupy no volume within the wing and power leads may be run along the external wing surfaces by electrically conducting tape. Such an easy installation means that multiple exciters may be quickly applied to hard points on test aircraft. By using multiple adaptive vanes, they may be driven by the same or different signals; but, more importantly, they may be phased so as to leverage excitation levels. Clearly, the development of such an advanced system will greatly enhance flutter testing through structural excitation. Accordingly, this study is centered on investigating the fundamental properties of this rotationally-active flutter test surface (RAFTS).

2. Technical Objectives

This investigation is centered on demonstrating the basic feasibility of the RAFTS exciter. As a first step, this study will establish the working principles of the RALA actuators within a scaled flutter test surface. As a funding option, a full-scale test article may also be constructed.

Table 2.1 Goals of RAFTS Project

i. Develop aerodynamic and structural models for RAFTS actuator vane
ii. Construct and bench-test a prototype RAFTS actuator vane for model verification

The first technical goal is set forth so that a new class of actuator vanes using the RALA actuators may be developed. To accomplish this, a series of vortex-lattice codes will be constructed for aerodynamic predictions. USAF DatCom methods will also be used for modeling under separated flow conditions. The structural models will be built upon laminated plate and virtual work theories as well as finite-element methods.

The second major goal is to bring a feasible RAFTS design to life. This new class of exciter vane will be first modeled on a 1/4 scale for verification of the structural models. A series of bench tests will confirm frequency response, moment generation capability and deflection levels. A funding option will be used for the construction of a full-scale exciter vane.

The first three months have yielded progress in two main areas on the Rotationally Adaptive Flutter Test Surface (RAFTS). The first area of advance is in aerodynamic modeling of the fin and selection of the preferred configuration. The second area involves structural modeling of rotational actuators and design of the active members.

3. Aerodynamic and Structural Modeling

3.1. Aerodynamic Modeling of Fin Candidates and Selection of Preferred Fin Configurations

As laid out in the kick-off meeting of 3/96, one of the major goals of the project is to maintain a level of control authority which is similar to existing flutter test surfaces. Accordingly, a fin with similar control capability was designed. By using the $N_{\delta f}$ requirements, Ref. 29 and Ref. 30, it was possible to arrive at a range of fin designs which would satisfy the normal force requirements. Because this work is initially being performed on a 1/2 scale vane, the normal force estimations were cut in proportion to the ratio of the areas (a factor of 4). Figure 1 shows the range of fin configurations which provide control increments which are similar to that those for the rotating-cylinder based structural excitation system (Ref. 3) at Mach 0.8 through 1.3. Because a second major design condition is the maintenance of low pitching moments, the maximum pitching moments were estimated for each design from Mach 0.8 to Mach 1.3. These moments were optimized by determining the hinge location which minimizes moments from 0 to 20° angle of attack. Figure 2 shows the results of the hinge moment determination for a given increment of lift slope. Clearly, the higher the aspect ratio, the higher the N_α and the lower the M_α. Accordingly, a fairly high aspect ratio airfoil was chosen with the limiting factor coming from aeroelastic and root bending moment considerations. Clearly, the main spar of this section should be formed from high strength composites or machined from high strength steel. Figure 3 shows the current configuration and outer mold lines for the RAFTS vane as obtained from aerodynamic optimization and force matching.

3.2. Structural Modeling of Rotational Actuators

A series of basic structural deformation estimations were derived from laminated plate theory and structural kinematics. By using the RALA configuration set forth Section 3 of the proposal, an expression for the cross-sectional area of the individual actuator was derived:

$$A = \frac{M \tan(\phi_{max})}{ELA^2} \tag{1}$$

Where A is the cross-sectional area, ø is the maximum rotation angle desired, E is the modulus of the active materials, L is the length of the material and Λ is the free-strain of the actuator strip. The rotator rod diameter is determined by Equation 2:

$$d = \frac{2L\Lambda}{\tan(\phi_{max})} \tag{2}$$

With these estimations, assuming piezoceramic lead zirconate titanate, PZT-5H at up to 220 μstrain over a 4" strip with ±1° of rotation, the rotator rod diameter is estimated to be 0.10" and the thickness of the active material strips is estimated at 0.033". Using 7.5 mil sheets to keep actuation voltages low, 5 layers of PZT will be required per actuator for the 50% scaled RAFTS surface.

3.3. Aerodynamic Force Matching

From the aerodynamic data presented in Ref. 29, it can be seen that the dynamic force in the transonic regime ranges from 52 to 65 lb peak-to-peak at 30,000 ft altitude. By using the aerodynamic data of Ref. 30 and 31, a map of minimum normal force slopes as a function of geometry may be obtained. If the geometries of Fig. 3.1 are used as a survey of candidate shapes, then their geometric parameters and aerodynamic characteristics through the transonic flight regime may be obtained:

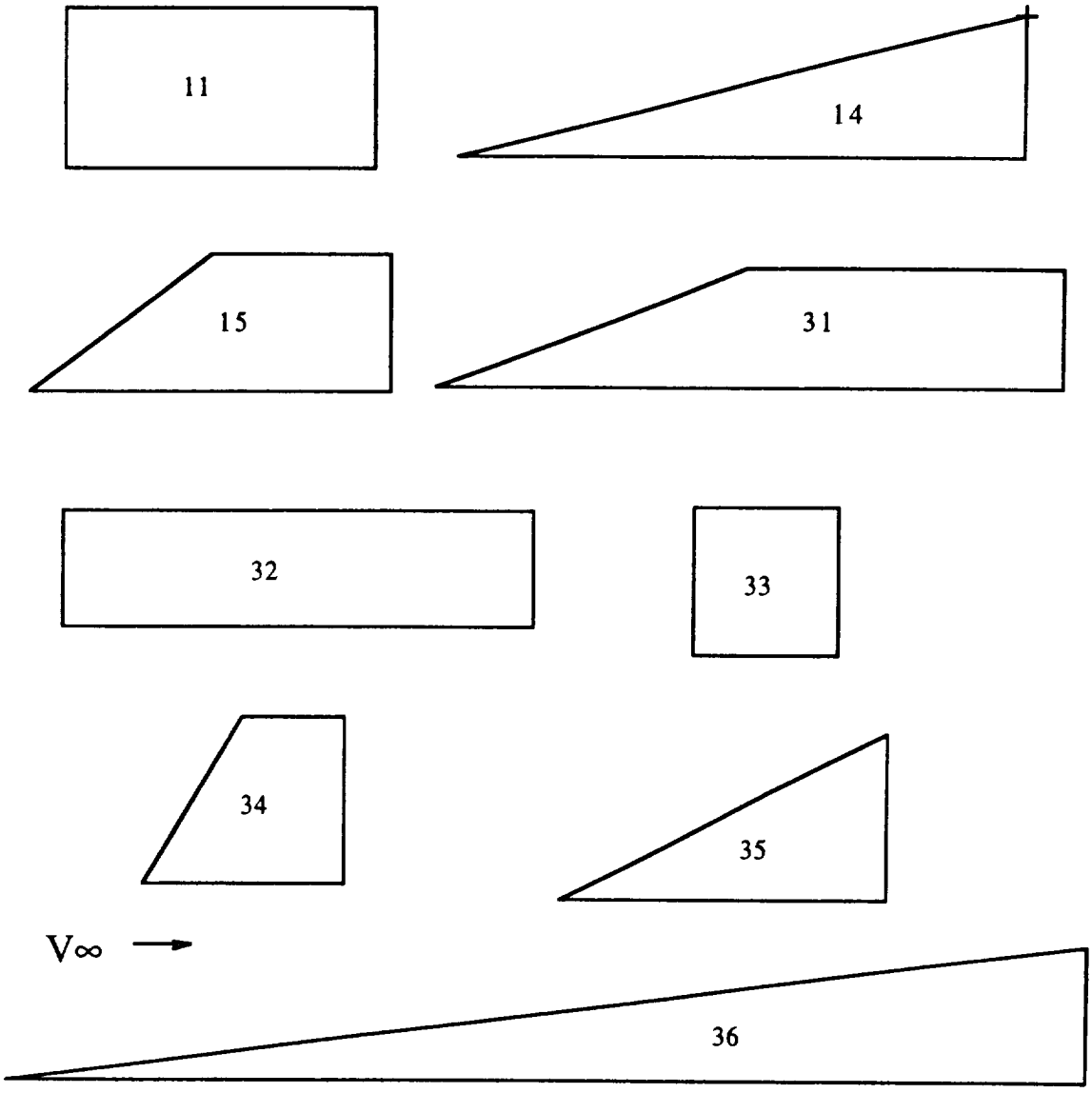

Figure 3.1 Candidate Vane Planforms

Table 3.1 Summary of Low Aspect Ratio Aerodynamic Surface Data, Mach 0.8 to 1.3

Config. No.	CNαmin (deg^-1)	Equivalent Full-Span Aspect Ratio	λ	ΔCLMmax
11	0.0225	1	1	0.044
14	0.0275	1	0	0.03
15	0.03	1	0.5	0.07
31	0.02	0.5	0.5	0.03
32	0.02	0.5	1	0.018
33	0.049	2	1	0.058
34	0.045	2	0.5	0.055
35	0.04	2	0	0.051
36	0.015	0.5	0	0.027

By using the above data, and assuming that the vane will be designed to generate peak-to-peak normal force variations of at least 52 lb at 30,000 ft, Mach 0.8, (282 psf dynamic pressure), the size and deflection range may be determined. From the data of Ref. 29, Fig. 12, it can be seen that the greatest transonic demands on the system in terms of normal force/dynamic pressure occur at Mach 0.8. Accordingly, the RAFTS vane actuator will be sized at this most stringent condition.

3.4. Size and Deflection Determination

To approximate the force levels generated by the DEI exciter vane, a $1ft^2$ area was selected as the initial starting reference point as it was approximately the same area as the DEI vane. By using the above information and assuming the 282 psf dynamic pressure, and taking the minimum value for $C_{n\alpha}$ (to be conservative), the deflection levels of the various vanes can be estimated. Table 3.2 summarizes the changes in angle of attack changes required for such a fin to generate normal force variations on the order of ±26 lbf at Mach 0.8, 30,000 ft.

Table 3.2 Summary of Minimum Aerodynamic Control and Geometric Parameters, Mach 0.8 - 1.3

Config. No.	Na (deg^-1)	Δα (1/2 p-p) (deg)	Cr (in)	Maximum ΔM (in-lbf)
11	6.345	4.10	17	211
14	7.755	3.35	34	287
15	8.46	3.07	22.6	446
31	5.64	4.61	32	270
32	5.64	4.61	24	122
33	13.818	1.88	12	196
34	12.69	2.05	15.6	243
35	11.28	2.30	24	345
36	4.23	6.15	48	365

From Table 3.2, it is clear that configuration #33 requires the least pitch change to generate the required ±26 lbf of normal force. Also, it has the second-lowest maximum change in total pitching moment from 0 to 20°, Mach 0.8 to Mach 1.3. Because of these characteristics, this simple configuration was selected as the configuration of choice.

The next logical step in the design of the vane is to choose the pivot point. To do this, a detailed look at the shift in center of pressure through the transonic regime is needed. From Ref. 30, a plot of c.p. migration from 0° - 12° at Mach 0.8 - 1.3 can be examined. Table 3.3 shows the changes experienced in center of pressure location as a function of angle of attack and Mach number.

Table 3.3 Chordwise Center of Pressure Location (%c) as a Function of Mach and Angle of Attack for Fin Configuration #33 (Square)

Alpha (deg)	.80	.85	.92	.98	1.10	1.20	1.30
.00							
.00	.450	.450	.450	.450	.450	.450	.450
4.00	.183	.200	.193	.258	.286	.300	.331
8.00	.206	.197	.219	.302	.350	.359	.364
12.00	.298	.265	.272	.330	.373	.372	.381
16.00	.367	.376	.378	.341	.377	.374	.398

By using the data of Table 3.3, and considering non-zero angles of attack, the location of the optimum hinge line may be determined. By examining the difference between the maximum and minimum pitching moment coefficients, a plot showing this change, ΔCLM, can illustrate the region where the lowest moment requirements occur, as shown in Figure 3.2.

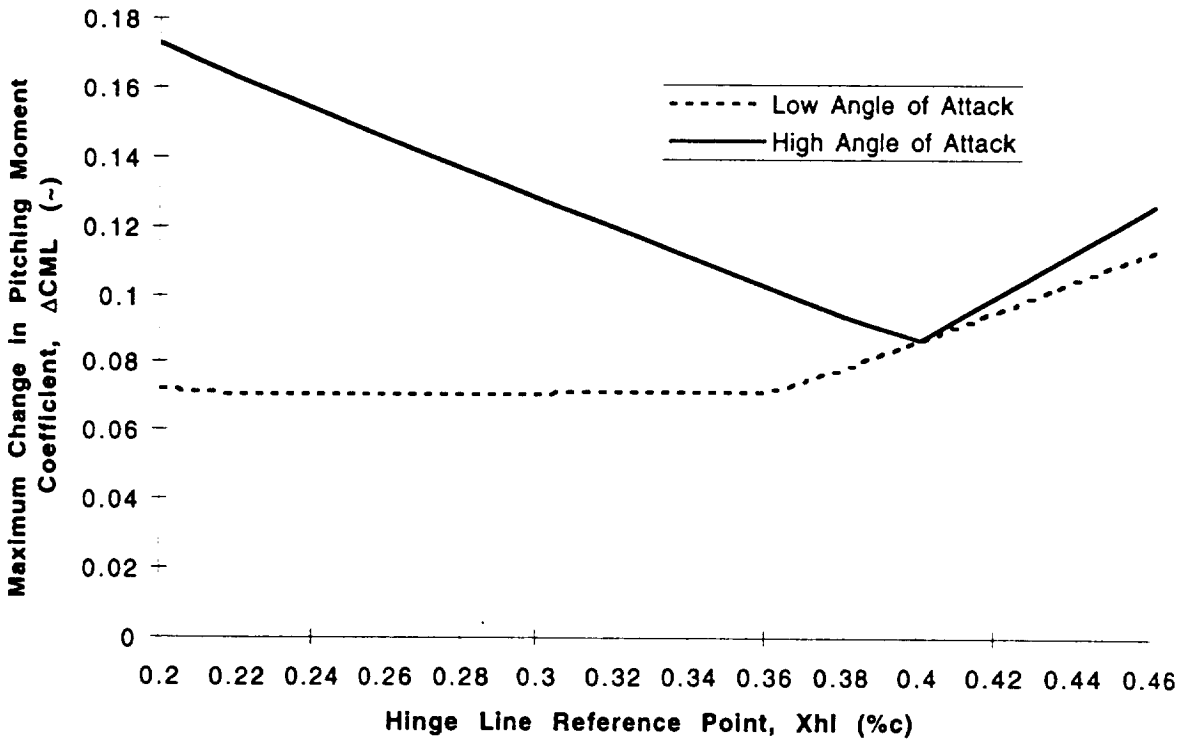

Figure 3.2 Maximum Change in Hinge Moment Coefficient in the Transonic Regime as a Function of Hinge Line Reference Point, Xhl (%c) for Fin Configuration #33 (Square)

From Fig. 3.2, it can be seen that there is a strong minimum in hinge moment coefficient with a 40%c hinge line in the high angle of attack condition. Because, however, the vane will generally be operating below 8° angle of attack, it is obvious that a hinge location from 23%c to 34%c has approximately the same net change in pitching moment coefficient. Accordingly, the hinge line will be placed at 33%c to keep the low angle of attach hinge moments low while approaching the minimum for the high angle of attack regime.

To match the hinge moments which the vane will encounter, the RALA actuators must be structurally balanced; accordingly, the actuator root width, Lr is one of the prime factors which determines the performance of the actuators. Considering a pair of 0.030" thick PZT actuators used top and bottom, with strain actuation capability ranging from -300 to 200μstrain, a rotation-deflection plot may be generated. Because the steady pitching moments are expected to range up to 120 lbf, it is clear that low-force, highly leveraged actuators will not be suitable. Figure 3 shows a map of actuator design parameters versus moment and deflection capability.

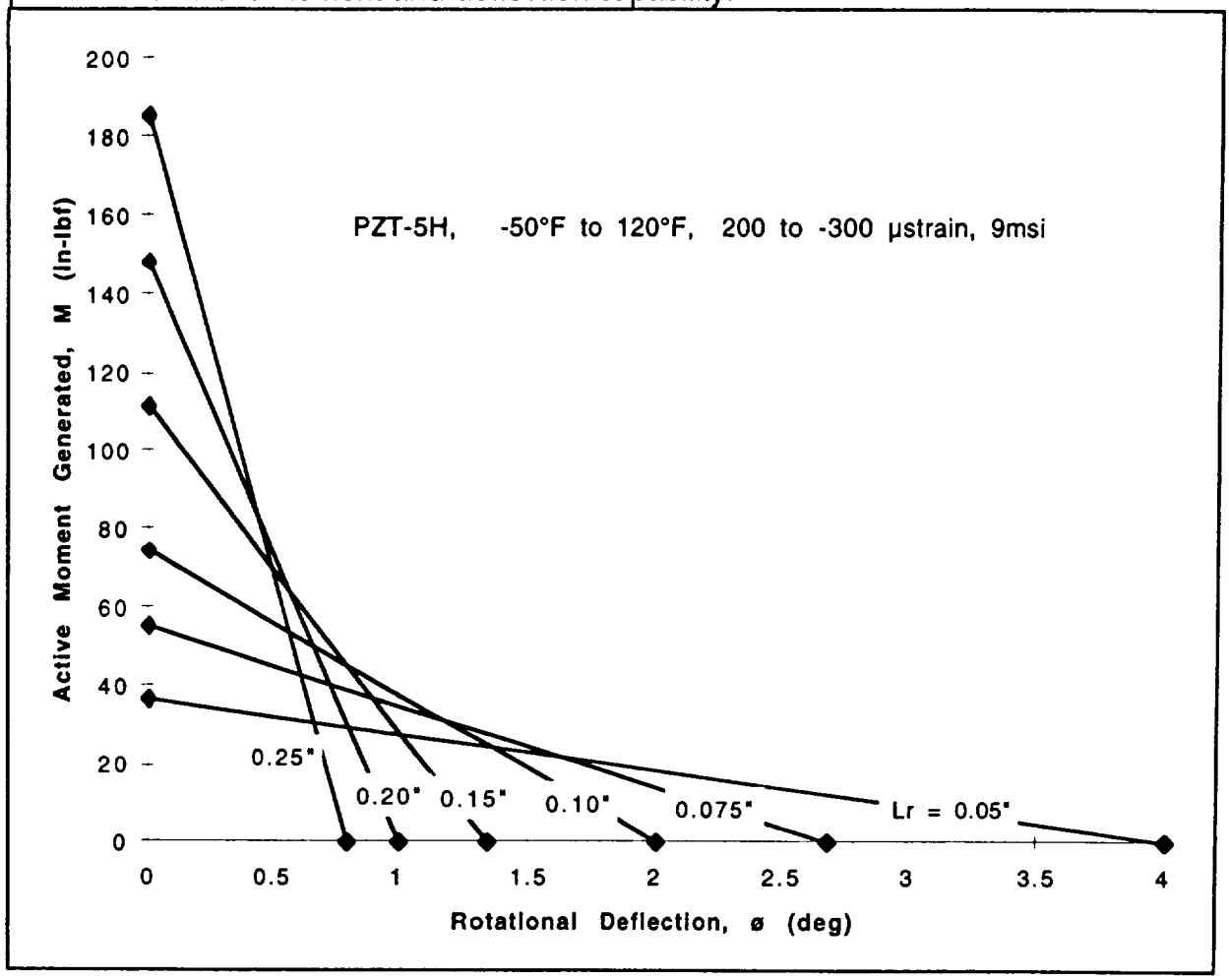

Figure 3.3 Rotational Deflection and Active Moments Generated by a 0.030" Thick RALA Actuator Configuration

From Fig. 3.3, considering the large pitching moments which the vane will experience, it is obvious that the root length should be 0.20" or greater. Unfortunately, this comparatively large dimension will effectively degrade deflections and accordingly, unsteady force levels. However, there are two mitigating factors to this seemingly discouraging result: 1) the -300 μstrain actuation level is approximately 1/2 of the maximum which may ultimately be obtained from PZT-5H, and 2), because RAFTS may be phased with respect to each other, their comparatively low force levels can be effectively magnified when multiples of the vanes are used in unison. One should note that the reason that the PZT-5H is not generally operated at the 600μstrain level is because of difficulties with arcing and cracking. However, it is highly likely that with better manufacturing techniques and stoichiometries of PZT, these limits may be safely crossed with little fear of structural failure.

Even with those mitigating factors, the large steady force levels will still pose problems for the RAFTS using current generation piezoceramics. In short, if the vanes were designed to generate large deflections, the strong, steady upwash or downwash field at the wing tip would simply drive the vanes against the rotation stops. There is, however, a configuration which would practically eliminate this problem. If the vane were allowed to rotate into the direction of the steady upwash field, then oscillate about the zero angle of attack range (instead of some comparatively large angle of attack), then the steady forces would be dropped by two or three orders of magnitude. To do this, a simple weathercock vane should be added to the system behind the front vane. Because the pivot is located at the 33%c, the most adverse nose-up moments will be generated in the high subsonic flight regime where the dynamic pressure is high, and yet the aerodynamic center is still located at the quarter-chord.

If a small 2" chord by 6" span vane is placed behind the forward vane, then the aerodynamic center of the entire system will be shifted aft. Using a main pivot location of 33%c with a 1 ft^2 forward vane followed by a 0.0833 ft^2 rear vane, the length of the rear vane level arm may be solved for by taking a very conservative system aerodynamic center of 50%c as exhibited by equation 1.

$$X_{ac} = \frac{\bar{X}_{acf} S_f C_{L\alpha f} + \bar{X}_{arf} S_r C_{L\alpha r}}{S_f C_{L\alpha f} + S_r C_{L\alpha r}} \tag{3}$$

where:

$Sf = 1\ ft^2$ $\quad Sr = 0.08333\ ft^2$ $\quad C_{L\alpha f} = 0.049 deg^{-1}$ $C_{L\alpha r} = 0.073 deg^{-1}$

$\bar{X}_{acf} = 0.33$ $\qquad \bar{X}_{ac} = 0.50$

The aerodynamic center location of the rear fin comes to:

$\bar{X}_{acr} = 2.5$ $\qquad X_{acr} = 30in$

With such an arrangement, the actuator system will possess positive stability throughout the flight envelope by at least 17%. Such a large static margin guarantees that the system will always rotate into the mean local flow field. From examination of the results of Ref. 29, it can be seen that the local flow field varies widely up to 15° at the wing tip (no doubt due to tip-vortex formation). Accordingly, the system stops must be placed far enough apart so as to permit the vane assembly to freely rotate up 15°. If it proves necessary in later tests, the stops in the assembly may be widened further. Appendix A shows the overall layout of the RAFTS system including the forward and rear weathercock vanes and the root mount.

3.5. Internal Structure Layout

The internal structure of the RAFTS forward adaptive vane is extremely simple. It consists of a pair of PZT sheets bonded to the main spar in the front and to each other in the back. The shell is connected to both points on the adaptive elements. These are clearly shown in Appendix A.

4. Fabrication and Testing

4.1. Mold Components and Vane Shell Fabrication

The components of the aluminum shell mold were completed and assembled. Following cutting, the mold was processed to provide a suitable release surface consisting of 2 mil thick Teflon sheets. More than two dozen different ply sequences were attempted till a suitable combination was achieved. Included in the lay-up sequence is a fiberglass protective outer layer, a lightning strike mesh, epoxy tape and the underlying graphite main structural skin. Enclosed figures in Appendix A detail more internal components of the shells.

4.2. Main Spar and Root Mount Fixtures

The second main group of components includes the base block, main spar, and mounting bar. These components were fabricated from aluminum and steel and form the structural core of the RAFTS vane. Enclosed figures show more detail on these components.

4.3. Tail Boom and Weathercock Vane

A graphite-epoxy composite tail boom and weathercock vane were also fabricated and bonded to the aft section of the RAFTS mounting bar. These components were co-cured in 350°F cures with Cyanimide 123 epoxy tape for superior strength and durability. Attached figures lay out more details of these structures.

4.4. Piezoceramic Actuators and Accelerometers

The final group of components to be fabricated is the piezoceramic actuator. This actuator is being constructed from PZT-5H sheets and will be matched to the anticipated amplifier, once available. In addition to integrating the PZT actuators into the shell structure, a pair of accelerometers are being integrated into the leading-edge of the RAFTS vane to provide pitch and bending information during flight. Attached figures in Appendix A show the overall geometry of the actuators.

4.5. Surface Work on the RAFTS Graphite Shell

The graphite shell on the RAFTS vane was taken from an unfinished state through Deflashing to a dimensionally conformal shape. Figure 4.1 shows the RAFTS shell just after removal from the molds.

Figure 4.1 RAFTS Shell Immediately Following Removal from Composite Tools, Prior to Deflashing

4.6. Integration of Main Spar and Piezoceramic Actuator Sheets

The steel spar was fitted to the piezoceramic actuator sheets in anticipation of the amplifier. Final assembly of the actuator element will have to wait till the amplifier becomes available so as to match dynamic impedance and mount only the number of elements which the amplifier is capable of driving. Towards this end, the first layers of piezoceramic actuator sheets were bonded to the substrate and main spar. Figure 4.2 shows the lay-up of the piezoceramic actuator sheets on the steel substrate.

Figure 4.2 Integration of Piezoceramic Sheets, Steel Substrate and Main Spar

4.7. Surface Finishing of the Weathercock Vane and Tail Boom

The surface finish of the weathercock vane and tail boom were worked on as well as a fit check. Figure 4.3 shows the structures after bonding, deflashing and surface finishing.

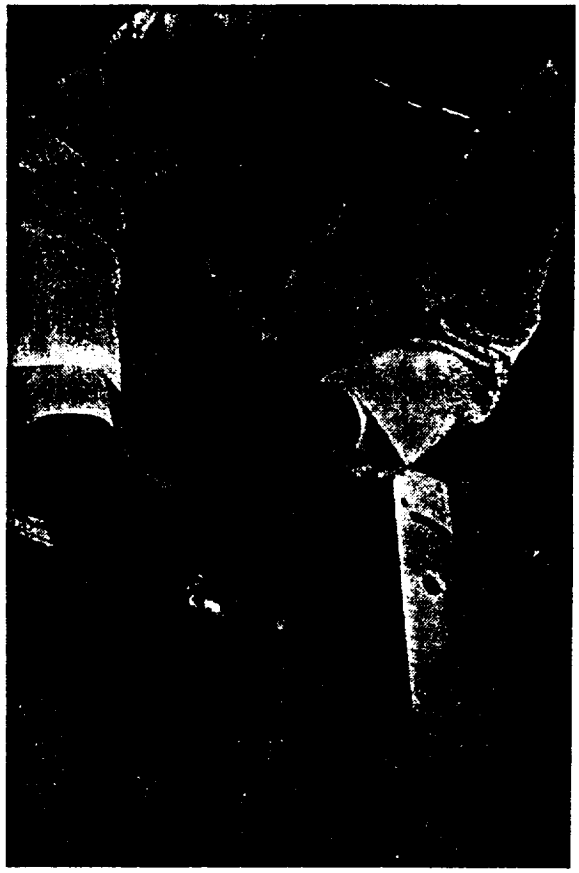

Figure 4.3 Weathercock Vane and Tail Boom Assembly

4.8 Testing

The RAFTS vane was structurally checked to 200 lbf of normal force with no sign of yielding. The load was applied to the main spar at the 14% semispan from the root fixture. Static testing showed 1.1 deg vane deflections with a corner frequency of 136 Hz and a natural frequency of 119 Hz as shown in Appendix B. Testing was executed with the use of a sine signal generator driving an ACX piezoelectric amplifier. Deflections were measured by Hall effect sensor and a National Instruments Data Acquisition System and checked by using laser reflection techniques.

5. Ground Test Instructions

5.1 Physical Description

The Rotationally Adaptive Flight Test Surface (RAFTS) vane is composed of several distinct groups of components. Descriptions of the components along with dimensions are contained in the attached pages. The base block acts as a mount for the entire structure and should be firmly attached to the airframe or test fixture. The six leads exit in the vicinity of the main spar bushing and should not be mechanically stressed.

Within the base block is a main spar bushing and steel main spar. These items firmly anchor the vane assembly to the base block. The main spar is attached to the piezoceramic actuator sheets via an internal insert and epoxy bond. The piezoceramic sheets are sandwiched in two stacks of four 7.5 mil thick PZT-5H sheets. The aft portion of the sheets is bonded to the aft of the RAFTS vane shell. The 30% chord of the shell is connected to the main spar through a Teflon-slip coating on the main spar itself. Although restrained from translating in any direction, the shell is able to freely rotate about the main spar as commanded by the piezoceramic actuators. At the base of the entire assembly is the vane mounting bar. This structure allows the vane too be pitched into the local freestream via the weather cock vane and tail boom assembly.

Instrumentation on the vane consists of two accelerometers mounted at the root and tip of the front portion of the forward vane bay. The main spar also bears strain gages at the root for arrangement in a typical cantilevered beam bridge.

5.2 Electrical Connections

A total of six wires exit the RAFTS vane. The forward blue wires bear accelerometer signals. The remaining four carry signals to and from the strain gages and piezoelectric actuators. These are shown schematically in Appendix C. They are listed below:

1. Blue outer accelerometer cable

This cable carries signals from the accelerometer mounted on the outer tip of the RAFTS vane.

2. Blue wire inner accelerometer

This cable carries signals from the accelerometer mounted on the inboard corner of the RAFTS vane.

3. Blue banded cable - two conductors

This cable carries two conductors with a grounded shielding. The blue conductor is attached to the top strain gage. The white conductor is attached to the bottom strain gage.

4. Blue banded cable - single conductor

This cable carries one conductor with a grounded shielding. The single conductor is connected to the center contact of both strain gages.

5. Red banded cable - two conductors

This cable carries two conductors with a grounded shielding. The two conductors have been soldered together and should be operated and tested in this condition. The inner contacts of the actuator stacks are connected to the two conductors. The reason why there are two conductors and not just one, is that for repoling operations, the leads will be desoldered and repoling fields may be applied independently to each of the stacks, i.e. it is a feature for maintenance and high-level testing.

6. Red banded cable - single conductor

This cable carries one conductor with a grounded shielding. The single conductor is connected to the outer contacts of both actuator stacks. Although this conductor is not grounded, it is closest in physical proximity to the main spar which is indeed grounded. If at all possible, this single conductor should also be grounded.

5.3 Operational Limits and Procedures

It is recommended that the PZT actuators be powered by sine waves at all times. If sine waves are unavailable, then duty-cycle balanced triangle waves will suffice. Square waves are to be avoided at all times. The actuation connections should be made between leads no. 5 and 6. The attached connection schematic shows the voltage and frequency range which is recommended. Static voltage limits should be set at ±115 VDC. These limits hold through 5 Hz. As the frequency is increased, the voltage should drop to ±50V at 100 Hz. No actuation is recommended beyond 200 Hz.

5.4 Testing

Deflections may be checked by using laser reflection techniques off the shell. Calibrated performance plots are also attached for both static and dynamic performance.

References

1. Bailey, T. and Hubbard, J. E., " Distributed Piezoelectric-Polymer Active Vibration Control of a Cantilever Beam," *Journal of Guidance, Control and Dynamics*, Vol. 8, No. 5, pp. 605-611, 1985.

2. Crawley, E. F. and De Luis, Javier, "Use of Piezoelectric Actuators as Elements of Intelligent Structures," *AIAA Journal*, Vol. 25, No. 10, Oct. 1987, pp. 987-997.

3. Crawley, E.F., Lazarus, K.B., and Warkentin, D. J., "Embedded Actuation and Processing in Intelligent Materials," *2nd Int. Workshop on Comp. Mat'ls and Struct.* Troy, NY.

4. Lazarus, K. B., Crawley, E. F., Bohlmann, J. D., "Static Aeroelastic Control Using Strain Actuated Adaptive Structures," proceedings of the First Joint U.S./Japan Conference on Adaptive Structures, Maui, Hawaii, October, 1990.

5. Song, O., Librescu, L. and Rogers, C. A., "Static Aeroelasticity Behavior of Adaptive Aircraft Wing Structures Modeled as Composite Thin-Walled Beams," presented at the International Forum on Aeroelasticity and Structural Dynamics, Aachen, Germany, June, 1991.

6. Ehlers, S. M., "Aeroelastic Behavior of an Adaptive Lifting Surface," Ph. D. Thesis, Purdue University, August, 1991.

7. Barrett, R. M., "Intelligent Rotor Blade and Structures Development Using Directionally Attached Piezoelectric Crystals," M.S. Thesis, University of Maryland, College Park, MD, May, 1990.

8. Barrett, R. M., "Intelligent Rotor Blade Actuation through Directionally Attached Piezoelectric Crystals," Presented at the *AHS National Forum, Washington, D.C., May 1990.*

9. Barrett, R. M., "Method and Apparatus for Structural Actuation and Sensing in a Desired Direction," *U. S. Patent Application 485,599/07*, 1990.

10. Barrett, R., "Active Plate and Missile Wing Development Using EDAP Elements," *Journal of Smart Materials and Structures*, Institute of Physics Publishing, Ltd., Techno House, Bristol, UK, Vol.1, No. 3, pp. 214-226, ISSN 096.

11. Barrett, R., "Active Plate and Missile Wing Development Using DAP Elements," *AIAA Journal*, March, 1994.

12. Barrett, R., "Aeroservoelastic DAP Missile Fin Development," *Journal of Smart Materials and Structures*, Institute of Physics Publishing, Ltd., Techno House, Bristol, UK, Vol. 2, No. 2, pp. 55-65, ISSN 0964-1726, June 1993.

13. Chen, P. and Chopra, I., "Feasibility Study to Build a Smart Rotor: Induced Strain Actuation of Airfoil Twist," From the *Proceedings of the 1993 North American Conference on Smart Materials and Structures,* Albuquerque, NM.

14. Barrett, R., "Modeling Techniques and Design Principles of a Low Aspect Ratio Active Aeroservoelastic Wing," *Proceedings of the North American Conference on Smart Materials and Structures,* Albuquerque, New Mexico, pp. 107 - 118, 1993.

15. Barrett, R., "Active Composite Torque-Plate Fins for Subsonic Missiles," paper presented at the Dynamic Response of Composite Structures Conference, New Orleans, Louisiana, August 30 - September 1, 1993.

16. Barrett, R., "Advanced Low-Cost Smart Missile Fin Technology Evaluation," Final Report to Wright Laboratory, USAF Armament Directorate, contract number F08630-93-C-0039 Eglin AFB, December, 1993.

17. Barrett, R., "All-Moving Active Aerodynamic Surface Research," presented at the 31st Annual Technical Meeting of the Society of Engineering Science, College Station, TX, October 10 - 12, 1994.

18. Barrett, R., "A Solid State Apparatus for Controlling Pitch Deflections of Aerodynamic Flight Control Surfaces," Auburn Univ. invention disclosure, October, 1994 (patent pending).

19. Barrett, R., Gross, R. S., and Brozoski, F., "Missile Flight Control using Active Flexspar Actuators," proceedings of the *1995 Smart Structures and Materials Conference,* February 26 - March 3, San Diego, California.

20. Barrett, R., Gross, R. S., and Brozoski, F. T., "Design and Testing of Subsonic All-Moving Smart Flight Control Surfaces," proceedings of the *36th AIAA Structures, Structural Dynamics and Control Conference,* New Orleans, LA, April, 1995, pp. 2289 - 2296, AIAA paper no. AIAA-95-1081.

21. Barrett, R., "Aeroservoelastic Characteristics of All-Moving Adaptive Flight Control Surfaces," paper presented at the 10th VPI & SU symposium on Dynamics and Control, 8 - 10 May, 1995.

22. Barrett, R., "Rotational Active Linear Actuators," Barrett Aerospace Technologies Invention Disclosure and Laboratory Report, September, 1995.

23. Kehoe, Michael W., "Aircraft Flight Flutter Testing at the NASA Ames-Dryden Flight Research Facility," NASA TM-100417, May 1988.

24. Norton, William J., "Random Air Turbulence as a Flutter Excitation Source," Proceedings of the 20th Annual Symposium, Society of Flight Test Engineers, Reno, Nevada, 1989, pp. 6.4-1 - 6.4-11.

25. Goldman, A., Rider, C.P., and Piperias, P., "Flutter Investigations on a Transavia PL12/T400 Aircraft," Aeronautical Research Laboratories, Melbourne, Australia, July 1989.

26. Van Nunen, J.W.G., and Piazzoli, G., "Volume 9: Aeroelastic Flight Test Techniques and Instrumentation," AGARD Flight Test Instrumentation Series, AG-1606, Feb. 1979.

27. Larue, P., Millet, M., and Piazzoli, G., "Pyrotechnic Bonkers for Structural Tests in Flight," La Recherche Aerospatiale, May-June 1974, pp. 137 - 146.

28. Vernon, Lura, "In-flight Investigation of a Rotating Cylinder-Based Structural Excitation System for Flutter Testing," NASA Technical Memorandum 4512, NASA Dryden Flight Research Facility, Edwards, California, 1993.

29. Mottinger, T. A., and Washington, W. D., "An Experimental Investigation of Low Aspect Ratio Fins Tested at Transonic Speeds on a Reflecting Plane," Aeroballistics Directorate, U.S. Army Missile Command, Redstone Arsenal, Alabama, Report No. RD-TM-71-15, July 1971.

30. Roskam, J., "Preliminary Calculation of Aerodynamic Characteristics," *Airplane Design,* published by Roskam Aviation and Engineering Corporation, Ottawa, KS 1990.

31. Vernon, L., "In-Flight Investigation of a Rotating Cylinder-Based Structural Excitation System for Flutter Testing," NASA TM 4512, 1993.

12. References

1. Bailey, T. and Hubbard, J. E., " Distributed Piezoelectric-Polymer Active Vibration Control of a Cantilever Beam," *Journal of Guidance, Control and Dynamics,* Vol. 8, No. 5, pp. 605-611, 1985.

2. Crawley, E. F. and De Luis, Javier, "Use of Piezoelectric Actuators as Elements of Intelligent Structures," *AIAA Journal,* Vol. 25, No. 10, Oct. 1987, pp. 987-997.

3. Crawley, E.F., Lazarus, K.B., and Warkentin, D. J., "Embedded Actuation and Processing in Intelligent Materials," *2nd Int. Workshop on Comp. Mat'ls and Struct.* Troy, NY.

4. Lazarus, K. B., Crawley, E. F., Bohlmann, J. D., "Static Aeroelastic Control Using Strain Actuated Adaptive Structures," proceedings of the First Joint U.S./Japan Conference on Adaptive Structures, Maui, Hawaii, October, 1990.

5. Song, O., Librescu, L. and Rogers, C. A., "Static Aeroelasticity Behavior of Adaptive Aircraft Wing Structures Modeled as Composite Thin-Walled Beams," presented at the International Forum on Aeroelasticity and Structural Dynamics, Aachen, Germany, June, 1991.

6. Ehlers, S. M., "Aeroelastic Behavior of an Adaptive Lifting Surface," Ph. D. Thesis, Purdue University, August, 1991.

7. Barrett, R. M., "Intelligent Rotor Blade and Structures Development Using Directionally Attached Piezoelectric Crystals," M.S. Thesis, University of Maryland, College Park, MD, May, 1990.

8. Barrett, R. M., "Intelligent Rotor Blade Actuation through Directionally Attached Piezoelectric Crystals," Presented at the *AHS National Forum, Washington, D.C., May 1990.*

9. Barrett, R. M., "Method and Apparatus for Structural Actuation and Sensing in a Desired Direction," *U. S. Patent Application 485,599/07,* 1990.

10. Barrett, R., "Active Plate and Missile Wing Development Using EDAP Elements," *Journal of Smart Materials and Structures*, Institute of Physics Publishing, Ltd., Techno House, Bristol, UK, Vol.1, No. 3, pp. 214-226, ISSN 096.

11. Barrett, R., "Active Plate and Missile Wing Development Using DAP Elements," *AIAA Journal,* March, 1994.

12. Barrett, R., "Aeroservoelastic DAP Missile Fin Development," *Journal of Smart Materials and Structures*, Institute of Physics Publishing, Ltd., Techno House, Bristol, UK, Vol. 2, No. 2, pp. 55-65, ISSN 0964-1726, June 1993.

13. Chen, P. and Chopra, I., "Feasibility Study to Build a Smart Rotor: Induced Strain Actuation of Airfoil Twist," From the *Proceedings of the 1993 North American Conference on Smart Materials and Structures,* Albuquerque, NM.

14. Barrett, R., "Modeling Techniques and Design Principles of a Low Aspect Ratio Active Aeroservoelastic Wing," *Proceedings of the North American Conference on Smart Materials and Structures,* Albuquerque, New Mexico, pp. 107 - 118, 1993.

15. Barrett, R., "Active Composite Torque-Plate Fins for Subsonic Missiles," paper presented at the Dynamic Response of Composite Structures Conference, New Orleans, Louisiana, August 30 - September 1, 1993.

16. Barrett, R., "Advanced Low-Cost Smart Missile Fin Technology Evaluation," Final Report to Wright Laboratory, USAF Armament Directorate, contract number F08630-93-C-0039 Eglin AFB, December, 1993.

17. Barrett, R., "All-Moving Active Aerodynamic Surface Research," presented at the 31st Annual Technical Meeting of the Society of Engineering Science, College Station, TX, October 10 - 12, 1994.

18. Barrett, R., "A Solid State Apparatus for Controlling Pitch Deflections of Aerodynamic Flight Control Surfaces," Auburn Univ. invention disclosure, October, 1994 (patent pending).

19. Barrett, R., Gross, R. S., and Brozoski, F., "Missile Flight Control using Active Flexspar Actuators," proceedings of the *1995 Smart Structures and Materials Conference*, February 26 - March 3, San Diego, California.

20. Barrett, R., Gross, R. S., and Brozoski, F. T., "Design and Testing of Subsonic All-Moving Smart Flight Control Surfaces," proceedings of the *36th AIAA Structures, Structural Dynamics and Control Conference*, New Orleans, LA, April, 1995, pp. 2289 - 2296, AIAA paper no. AIAA-95-1081.

21. Barrett, R., "Aeroservoelastic Characteristics of All-Moving Adaptive Flight Control Surfaces," paper presented at the 10th VPI & SU symposium on Dynamics and Control, 8 - 10 May, 1995.

22. Barrett, R., "Rotational Active Linear Actuators," Barrett Aerospace Technologies Invention Disclosure and Laboratory Report, September, 1995.

23. Kehoe, Michael W., "Aircraft Flight Flutter Testing at the NASA Ames-Dryden Flight Research Facility," NASA TM-100417, May 1988.

24. Norton, William J., "Random Air Turbulence as a Flutter Excitation Source," Proceedings of the 20th Annual Symposium, Society of Flight Test Engineers, Reno, Nevada, 1989, pp. 6.4-1 - 6.4-11.

25. Goldman, A., Rider, C.P., and Piperias, P., "Flutter Investigations on a Transavia PL12/T400 Aircraft," Aeronautical Research Laboratories, Melbourne, Australia, July 1989.

26. Van Nunen, J.W.G., and Piazzoli, G., "Volume 9: Aeroelastic Flight Test Techniques and Instrumentation," AGARD Flight Test Instrumentation Series, AG-1606, Feb. 1979.

27. Larue, P., Millet, M., and Piazzoli, G., "Pyrotechnic Bonkers for Structural Tests in Flight," La Recherche Aerospatiale, May-June 1974, pp. 137 - 146.

28. Vernon, Lura, "In-flight Investigation of a Rotating Cylinder-Based Structural Excitation System for Flutter Testing," NASA Technical Memorandum 4512, NASA Dryden Flight Research Facility, Edwards, California, 1993.

29. Mottinger, T. A., and Washington, W. D., "An Experimental Investigation of Low Aspect Ratio Fins Tested at Transonic Speeds on a Reflecting Plane," Aeroballistics Directorate, U.S. Army Missile Command, Redstone Arsenal, Alabama, Report No. RD-TM-71-15, July 1971.

30. Roskam, J., "Preliminary Calculation of Aerodynamic Characteristics," *Airplane Design,* published by Roskam Aviation and Engineering Corporation, Ottawa, KS 1990.

31. Vernon, L., "In-Flight Investigation of a Rotating Cylinder-Based Structural Excitation System for Flutter Testing," NASA TM 4512, 1993.

Appendix A

RAFTS Vane Figures

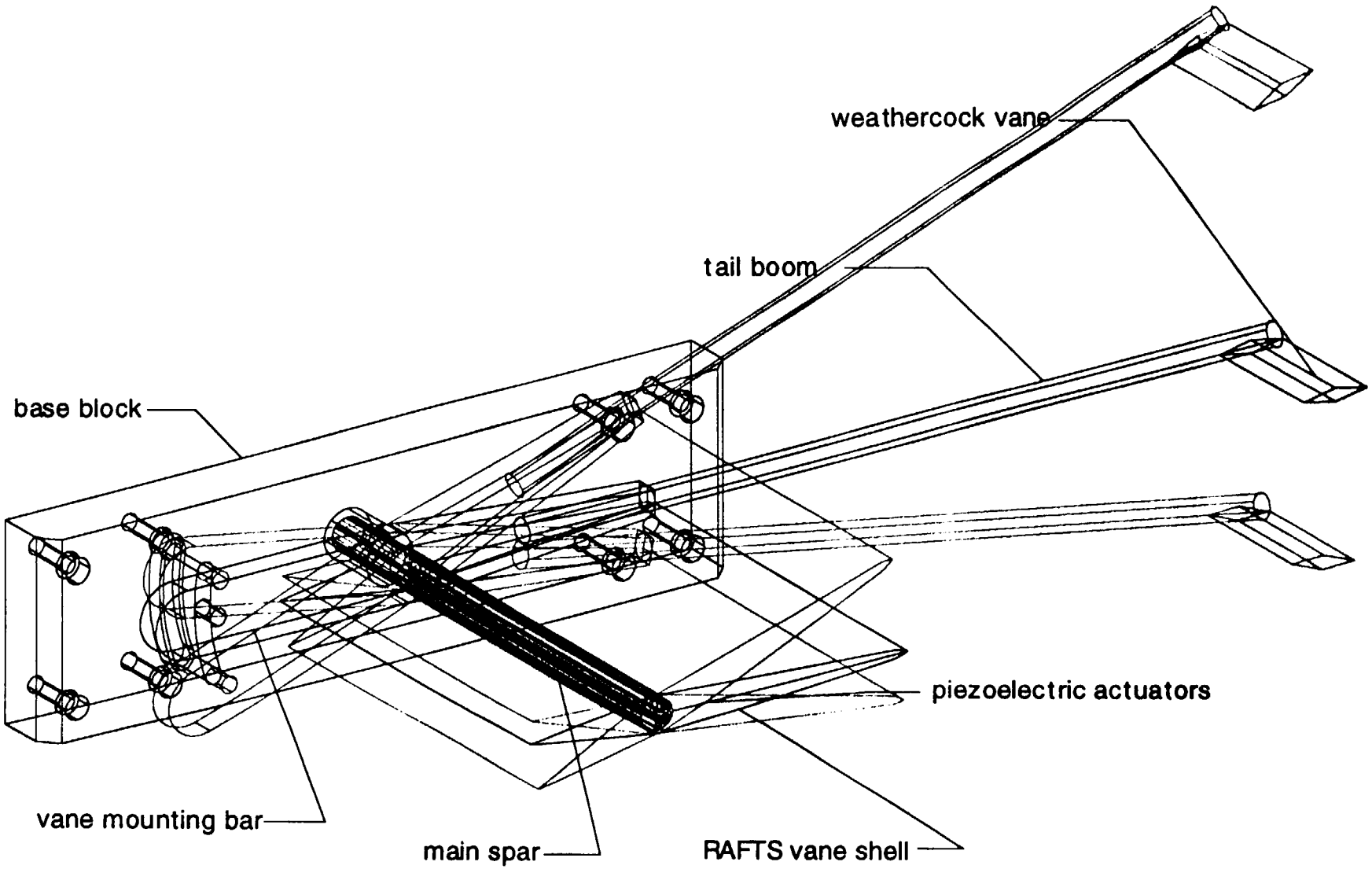

6" RAFTS Vane Assembly	Dr. By: R. Barrett	Date: 16 Oct. 1996	scale: 1/2	sheet 1/7

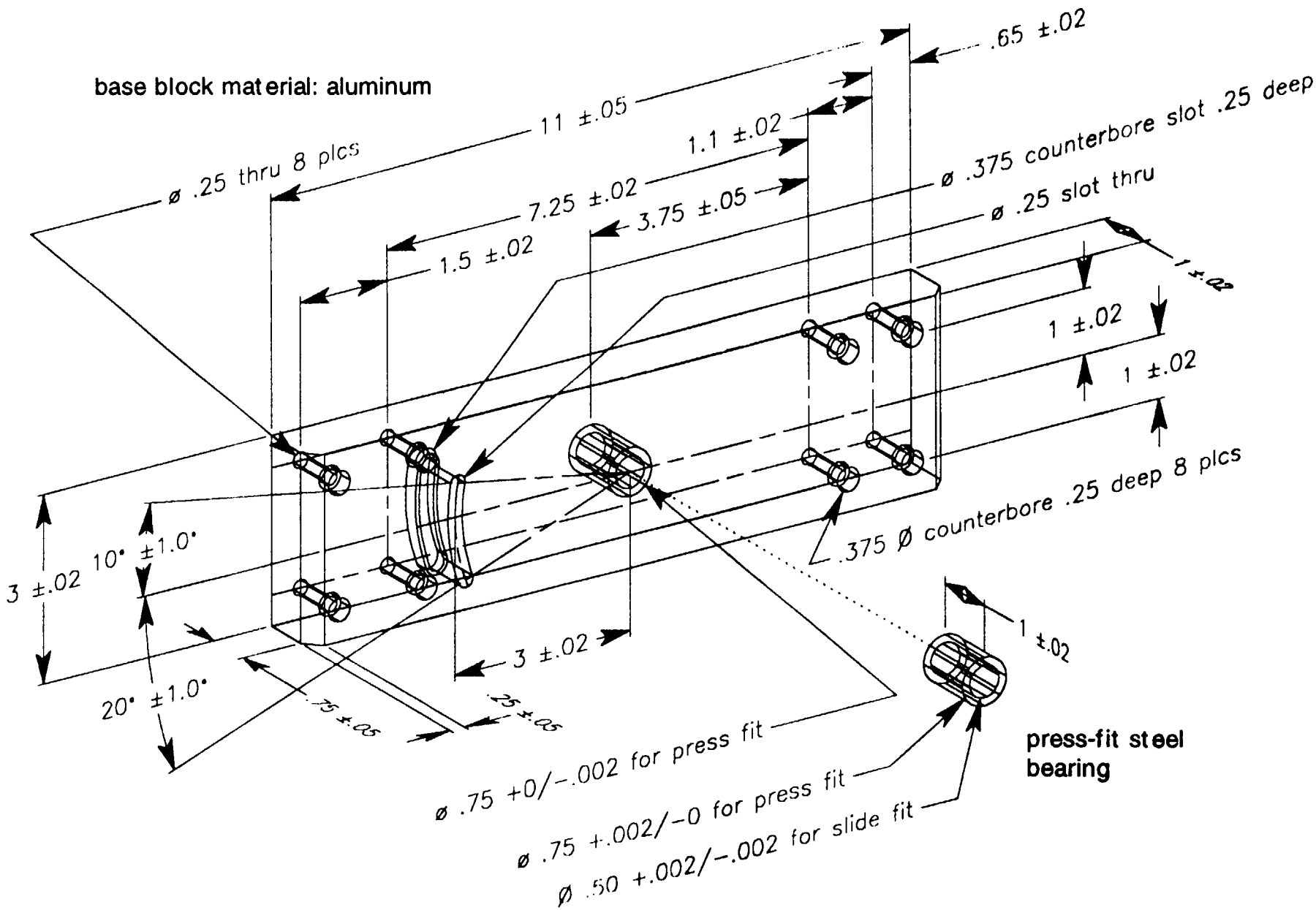

6" RAFTS Base Block	Dr. By: R. Barrett	Date: 16 Oct. 1996	scale: 1/2	sheet 2/7

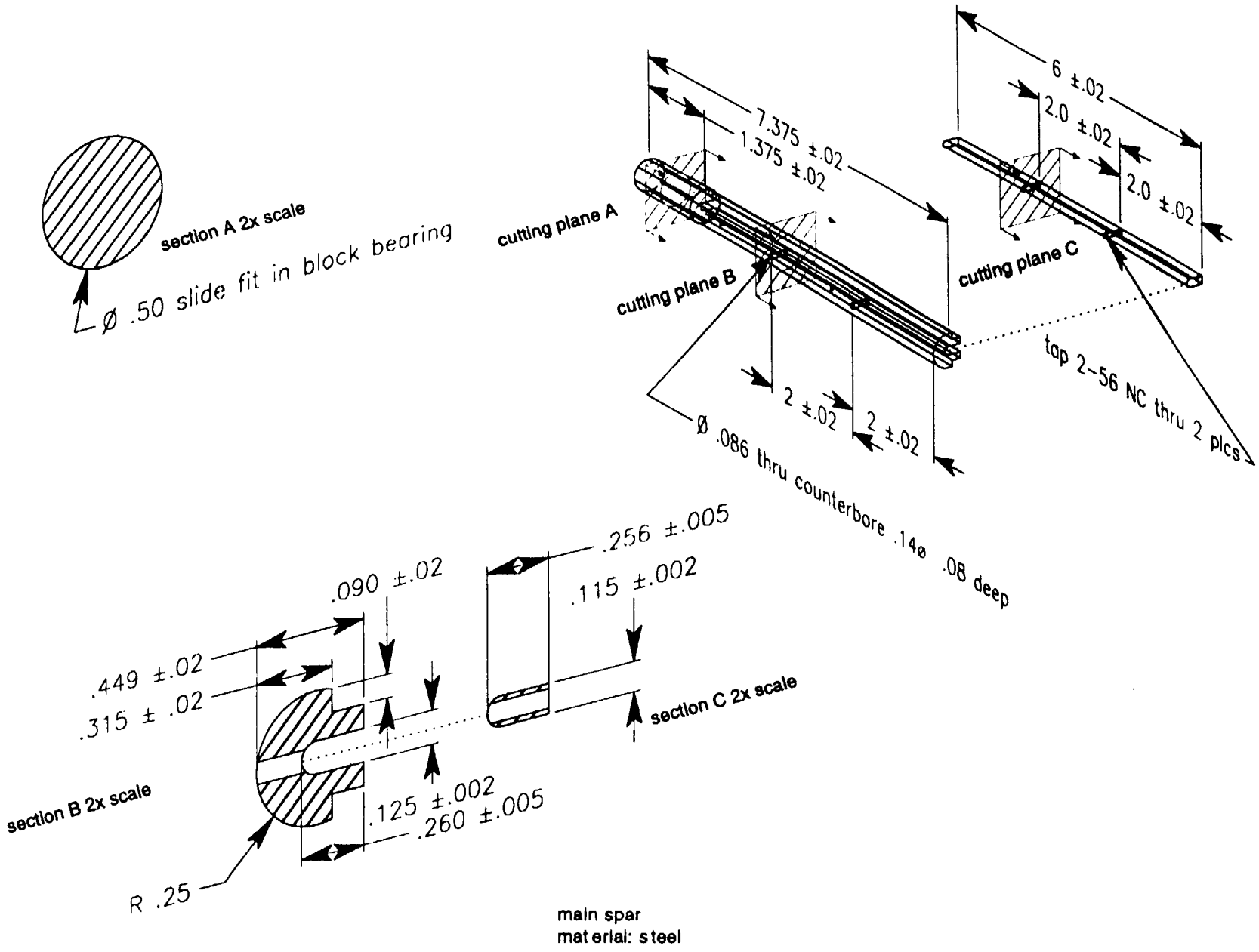

main spar
material: steel

6" RAFTS Main Spar	Dr. By: R. Barrett	Date: 16 Oct. 1996	scale: 1/2	sheet 3/7

tail boom
material: graphite/epoxy

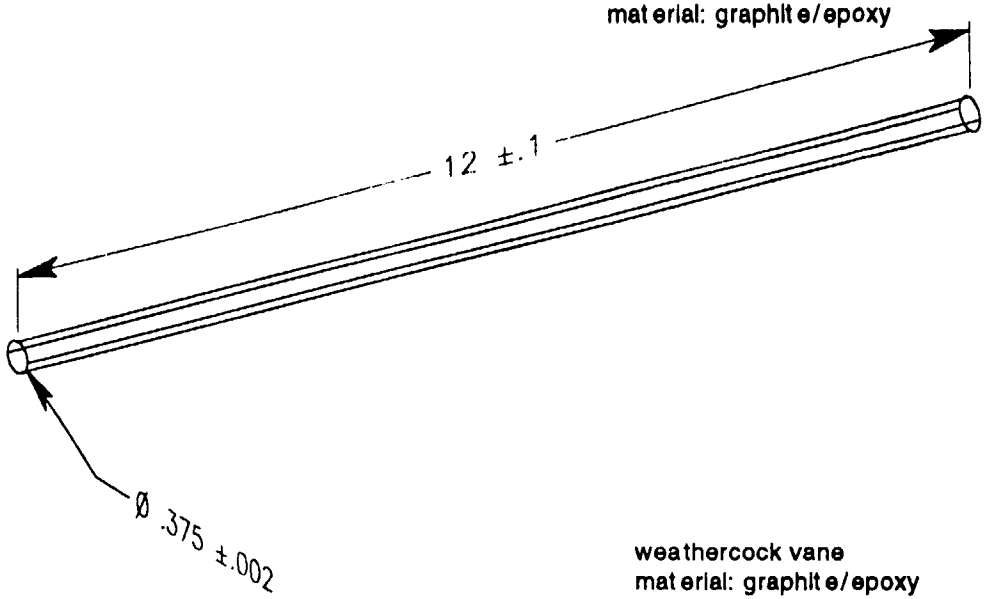

weathercock vane
material: graphite/epoxy

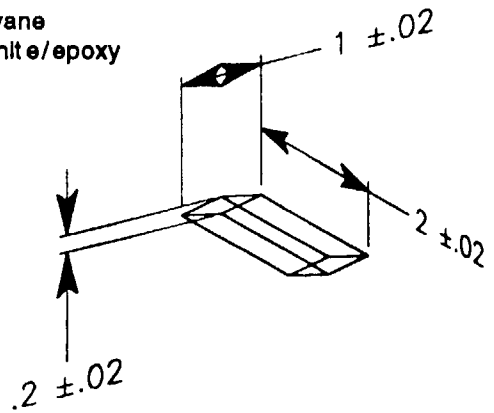

6" RAFTS Tail Boom Assembly	Dr. By: R. Barrett	Date: 16 Oct. 1996	scale: 1/2	sheet 4/7

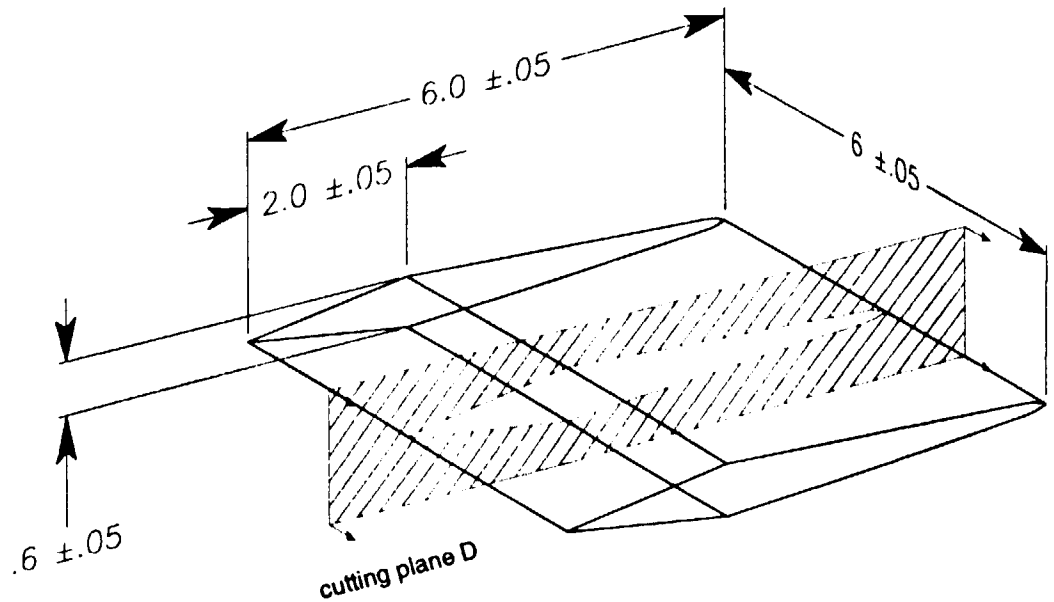

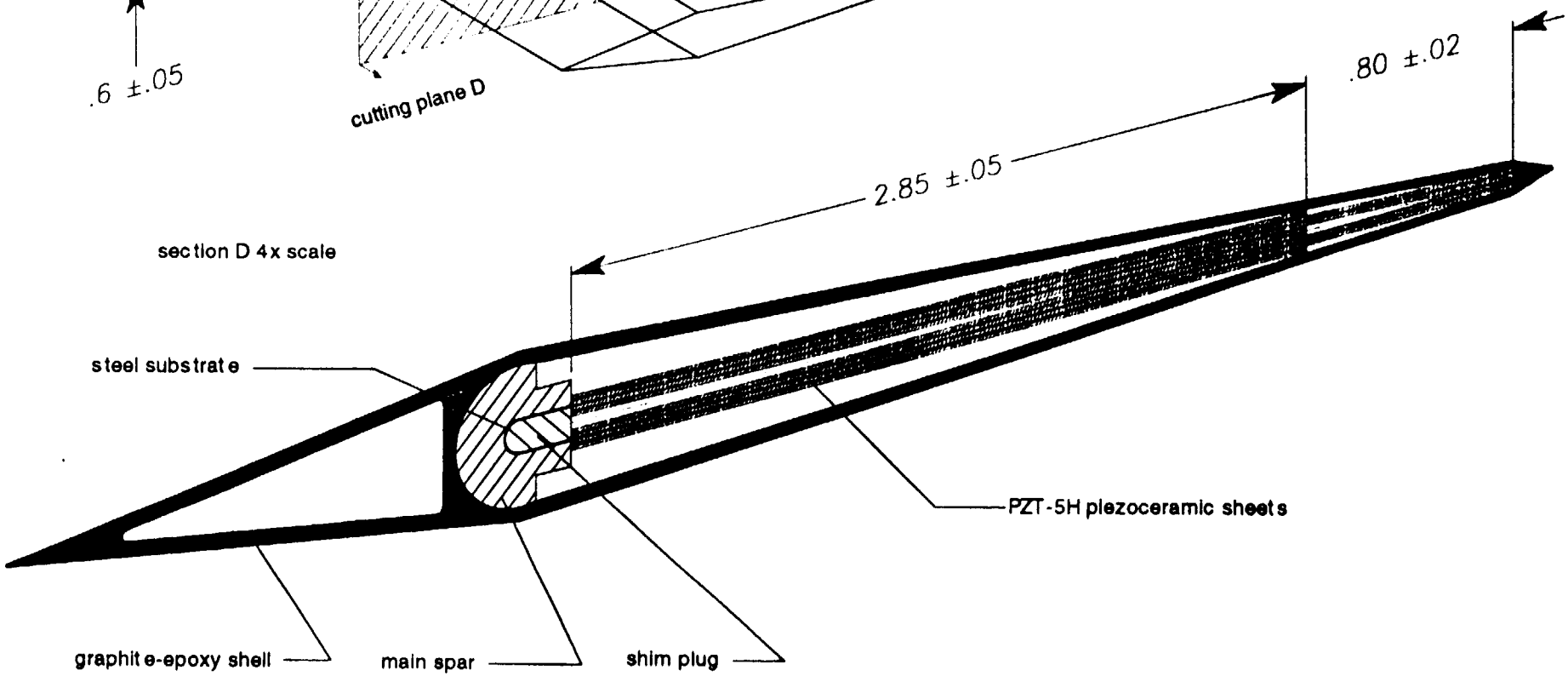

6" RAFTS Vane Shell	Dr. By: R. Barrett	Date: 16 Oct. 1996	scale: 1/2	sheet 5/7

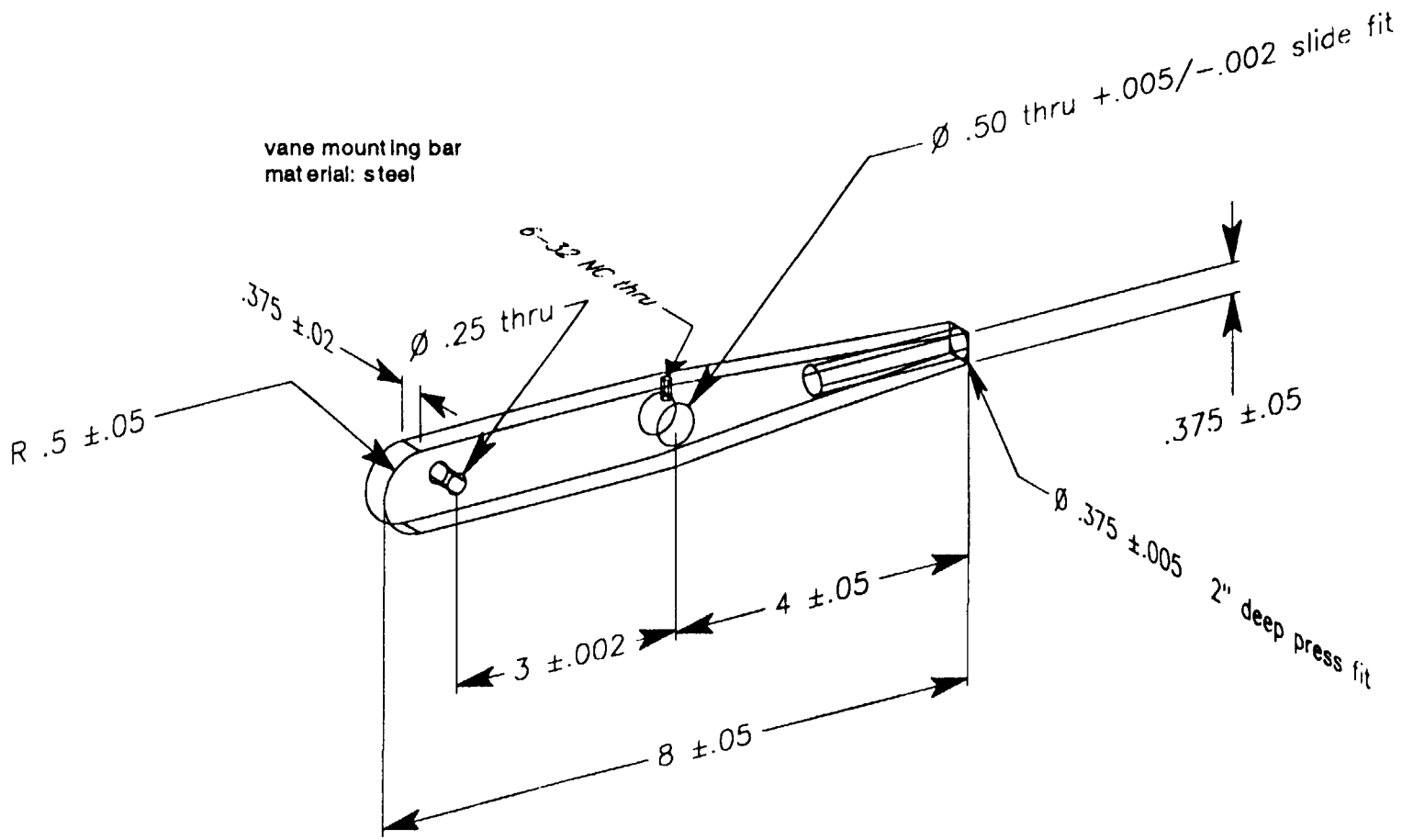

6" RAFTS Mounting Bar	Dr. By: R. Barrett	Date: 16 Oct. 1996	scale: 1/2	sheet 6/7

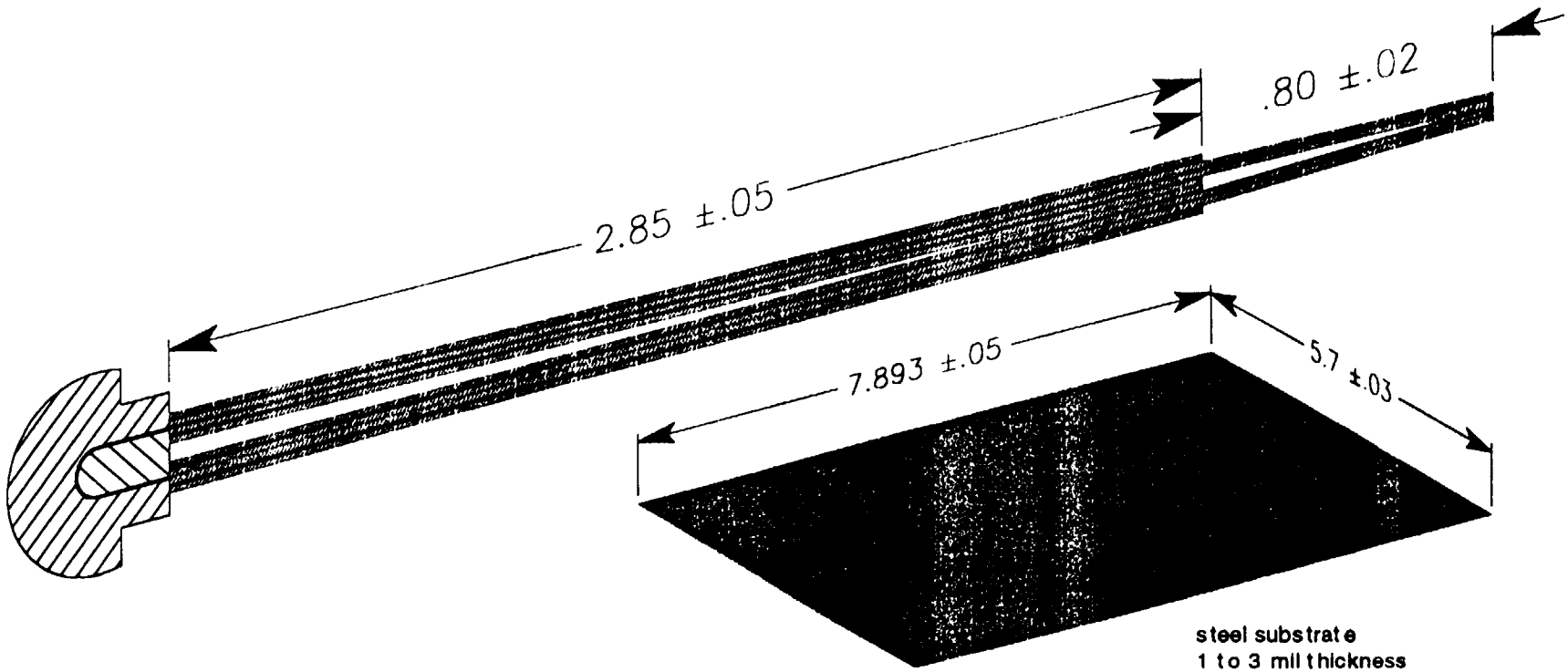

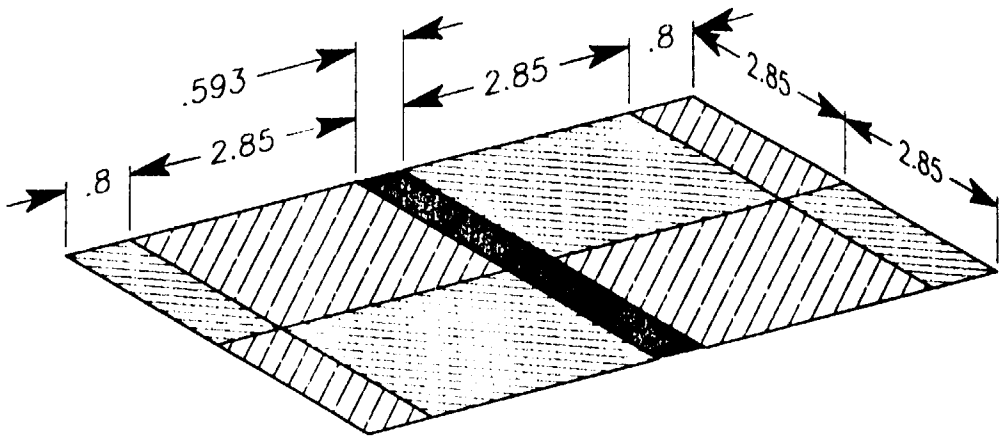

6" RAFTS Vane Shell	Dr. By: R. Barrett	Date: 16 Oct. 1996	scale: 1 /2	sheet 7 /7

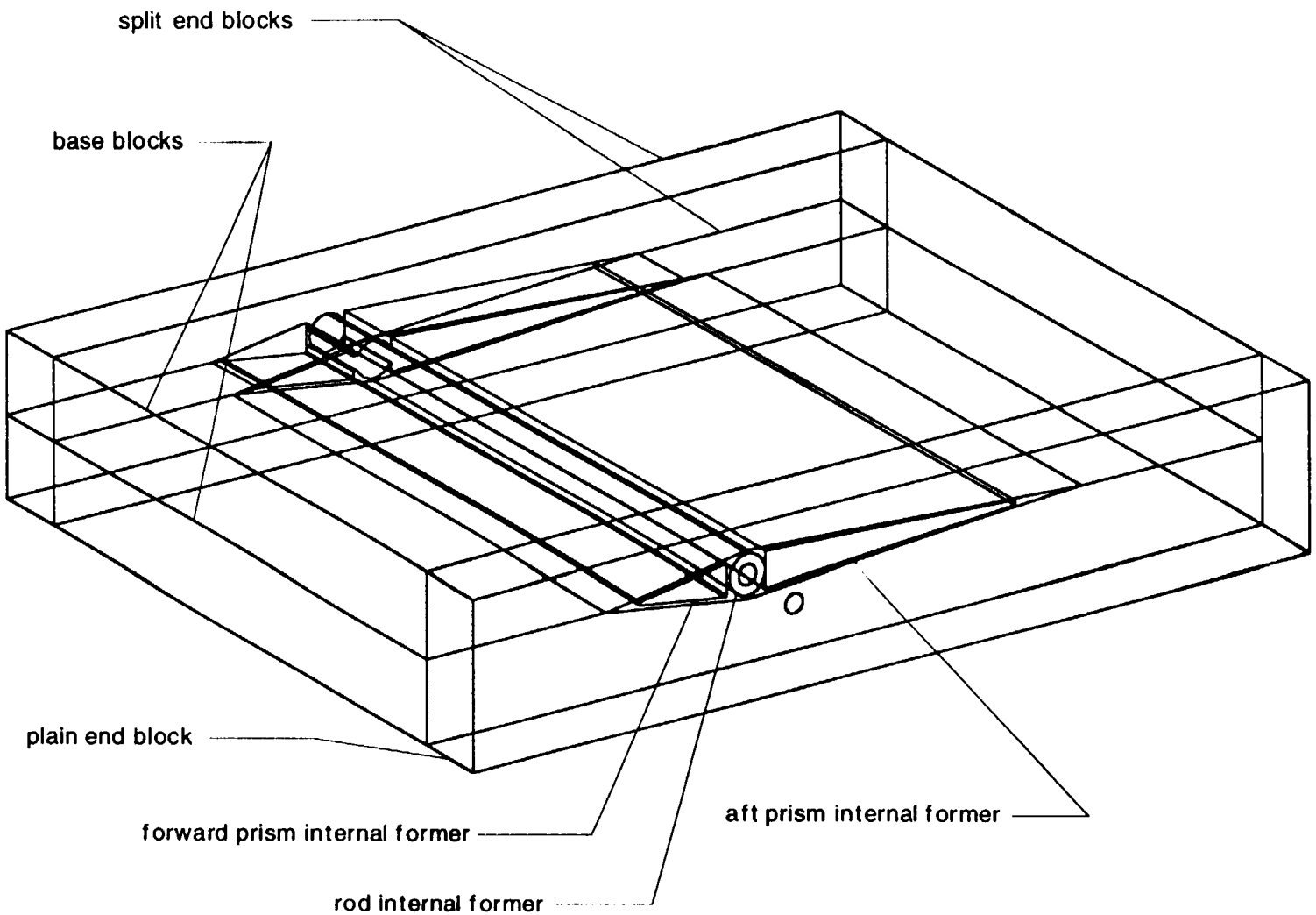

RAFTS Vane Mold Assembly	Dr. By B. Barrett	date: 15 October 1996	scale scale: 1/2	sheet 1/5

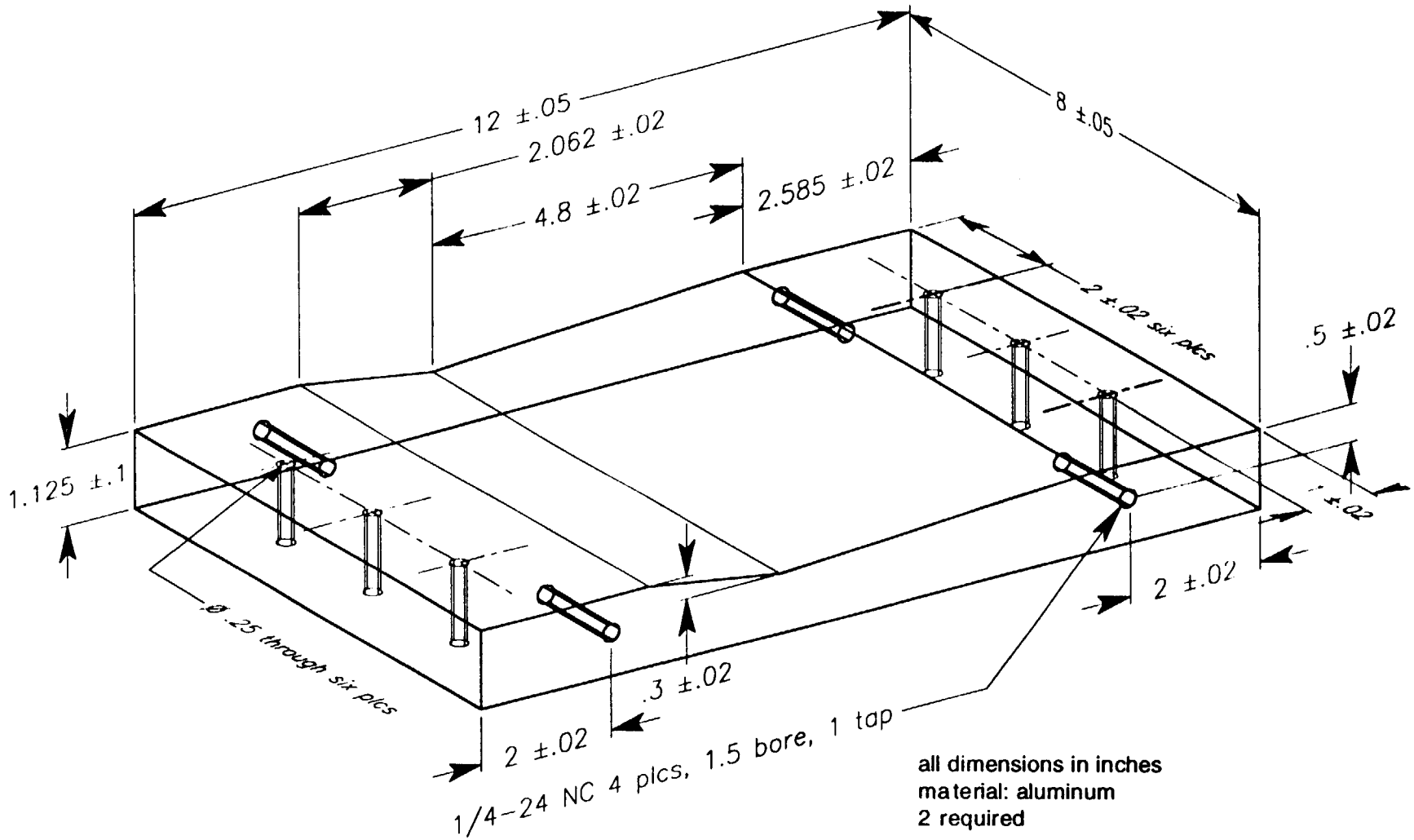

all dimensions in inches
material: aluminum
2 required

RAFTS Vane Mold Base Block	Dr. By R. Barrett	date: 15 October 1996	scale: 1/2	sheet 2/5

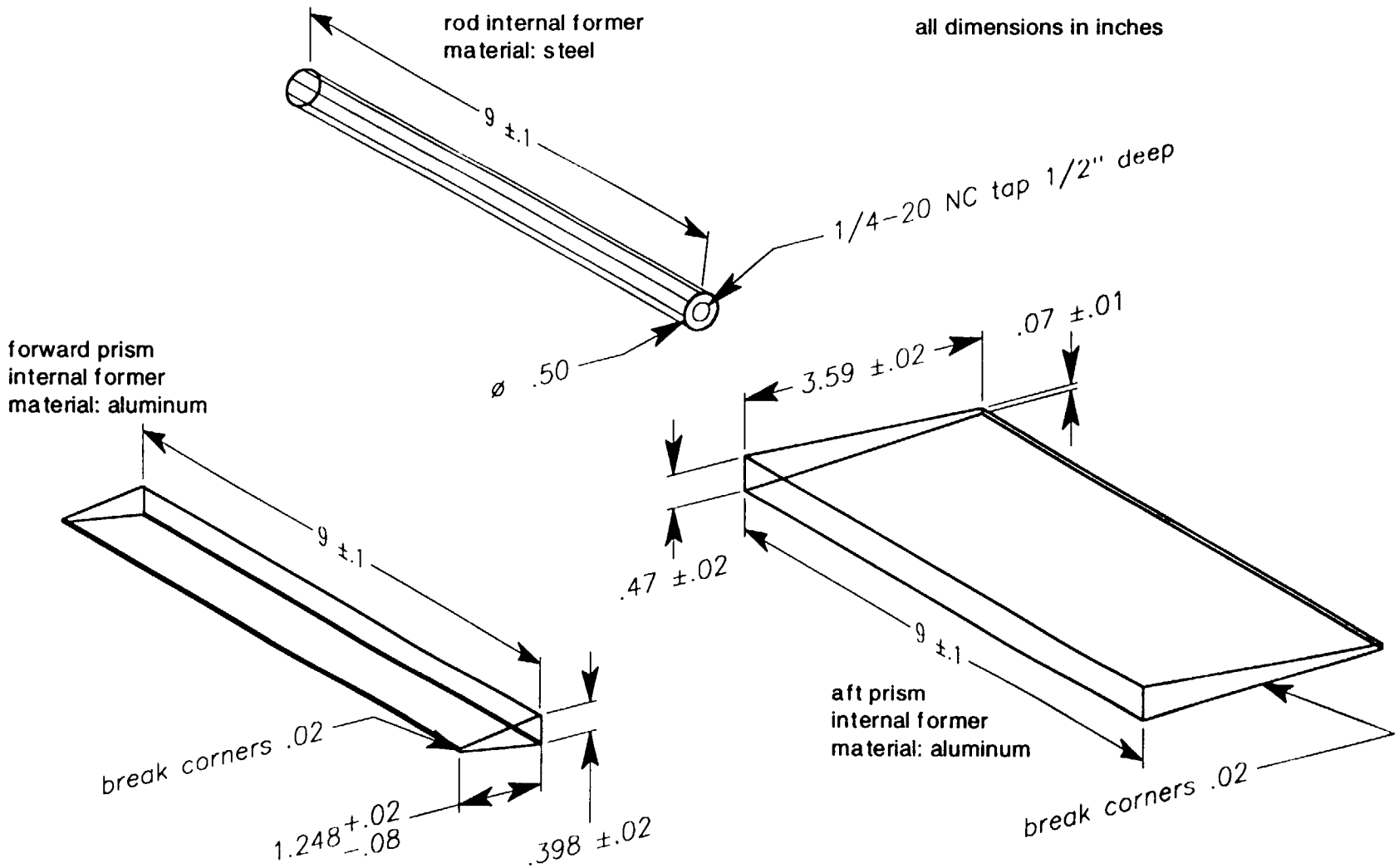

RAFTS Vane Mold Internal Formers	Dr. By R. Barrett	date: 15 October 1996	scale: 1/2	sheet 3/5

all dimensions in inches
material: aluminum
2 rq'd

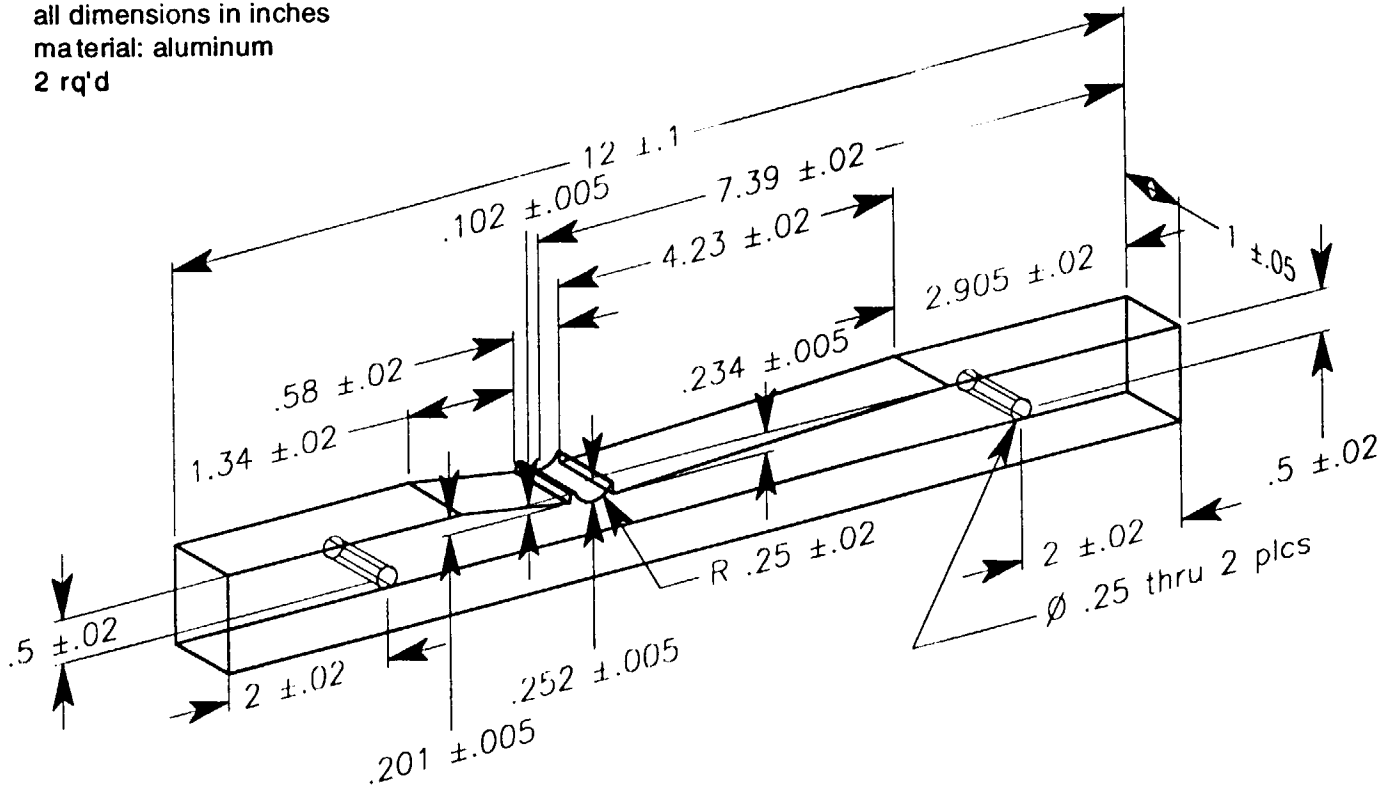

RAFTS Vane Mold Split End Blocks	Dr. By R. Barrett	date: 15 October 1996	scale: 1/2	sheet 4/5

all dimensions in inches
material: aluminum
1 rq'd

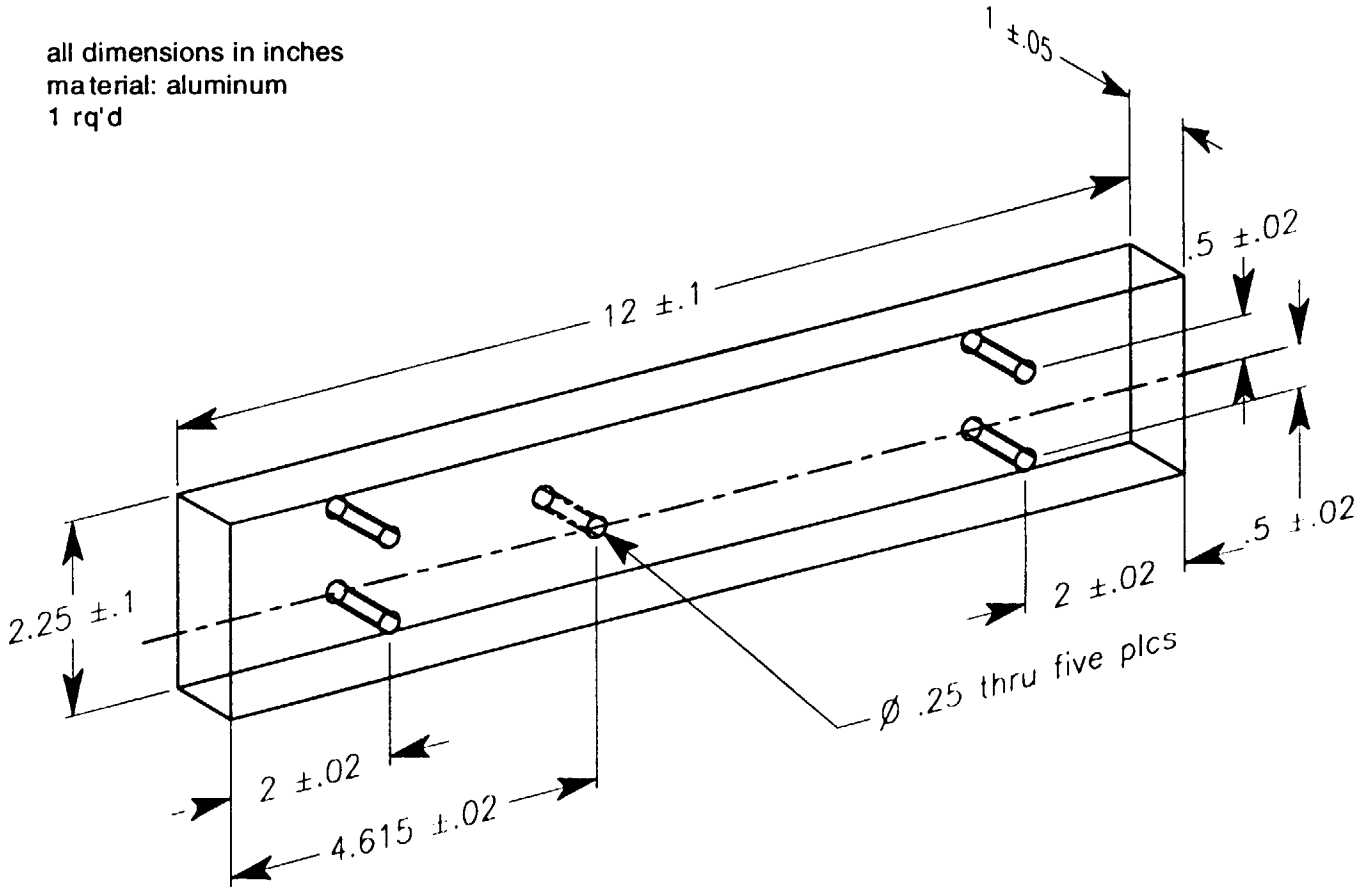

RAFTS Vane Mold Plain End Block	Dr. By R. Barrett	date: 15 October 1996	scale: 1/2	sheet 5/5

Appendix B

RAFTS Test Data

Static RAFTS Actuator Tip Pitch Deflection with Shell Removed

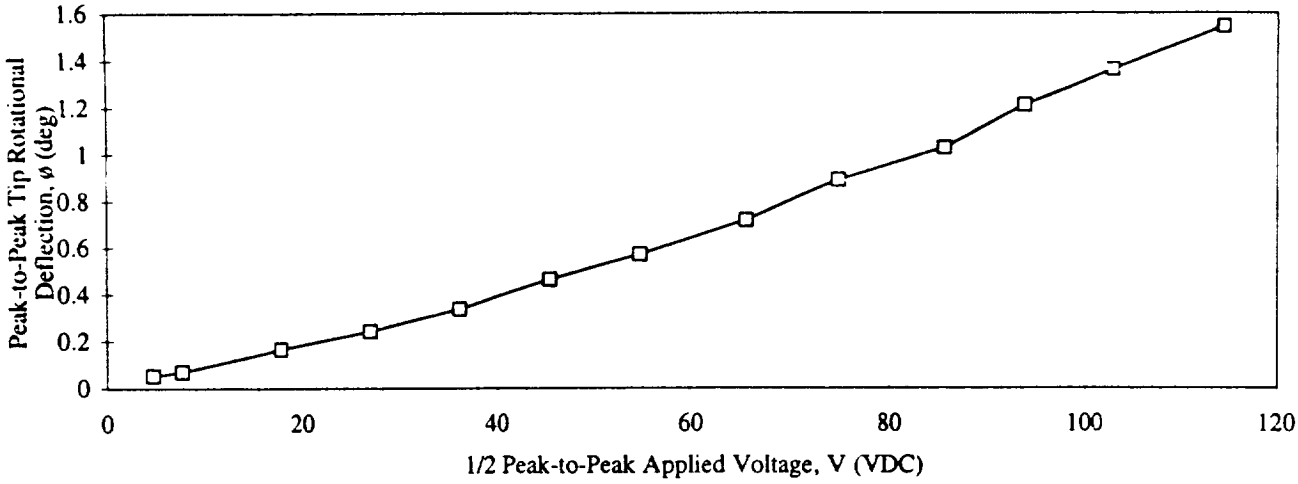

Static RAFTS Vane Pitch Deflection

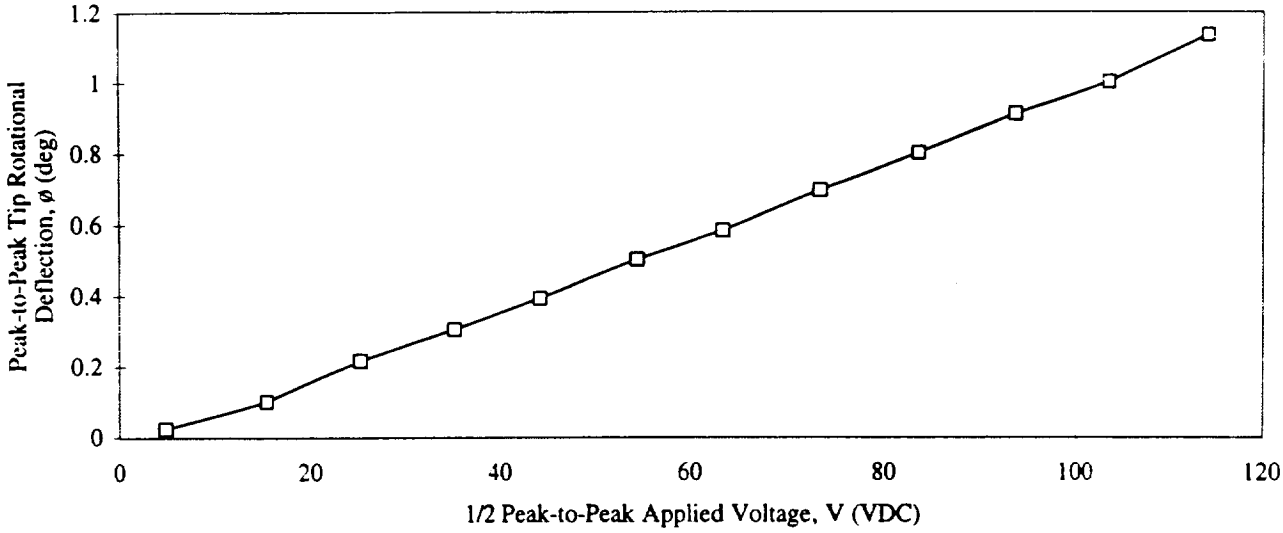

Dynamic RAFTS Vane Pitch Deflection

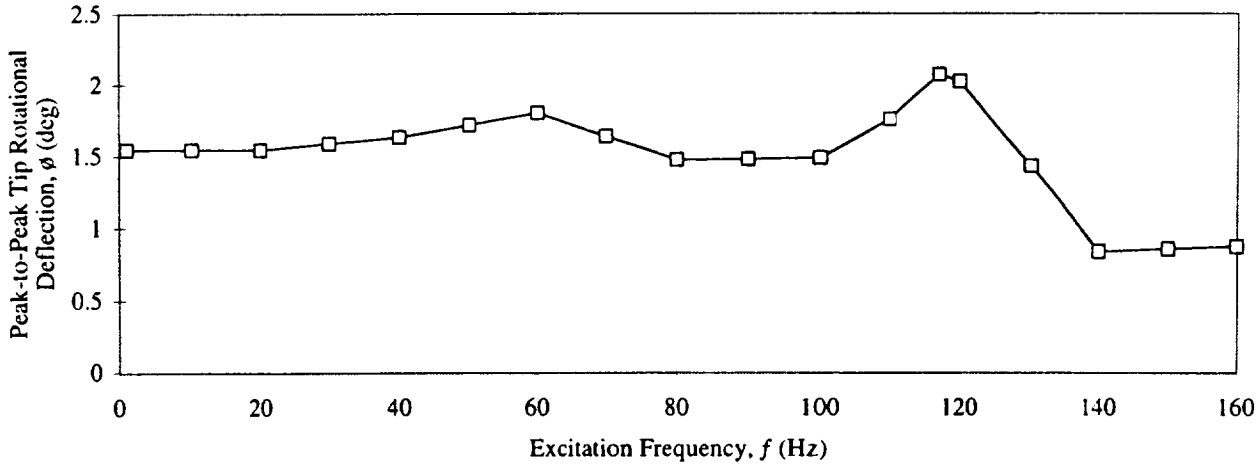

Appendix C

RAFTS Connection Schematic

Connection Schematic for RAFTS Vane

Cable 1 Blue
Outer Accelerometer

Cable 2 Blue
Inner Accelerometer

Cable 3 Blue banded two conductor cable
outer strain gage contacts

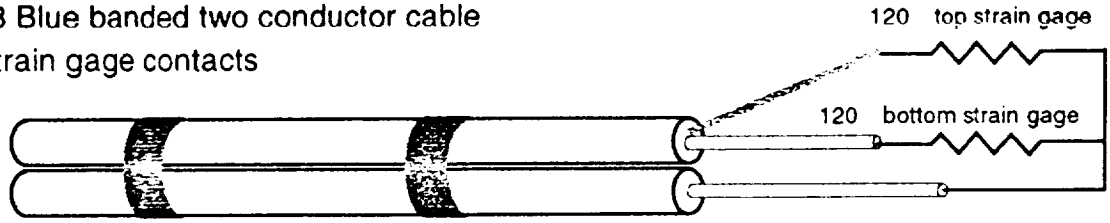

Cable 4 Blue banded single conductor cable
inner center strain gage contact

note: These two conductors should be connected for normal operation. They are separate only for maintenance and advanced testing purposes.

Cable 5 Red banded two conductor cable
outer strain gage contacts

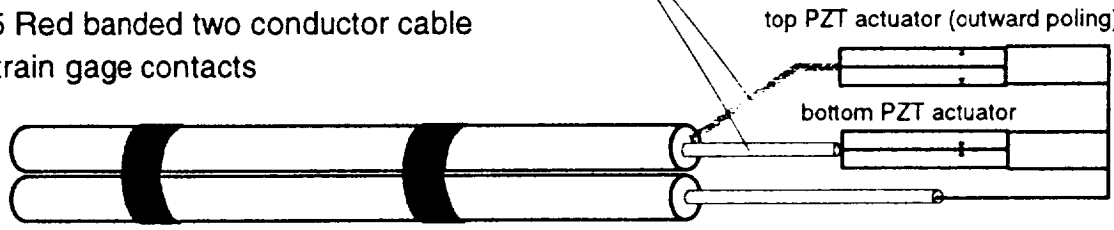

Cable 6 Red banded single conductor cable
inner center strain gage contact